

Modeling and Control of Side Face Beam Cracking

by Robert J. Frosch

As the use of thicker concrete covers has been increasing due to durability concerns, the question arises whether current design provisions for the control of side-face cracking remain applicable. This study investigates the background for the existing provisions and develops a physical model and procedure for the calculation of side-face crack widths. The calculation procedure is supported by an evaluation of existing test data. Based on this procedure, analyses are conducted that investigate side-face crack width profiles as well as parameters necessary to control side-face cracking for varying concrete covers. Design recommendations are presented that provide a unified approach to the control of side-face cracking as well as bottom-face cracking.

Keywords: beam; crack-control reinforcement; cracking.

INTRODUCTION

The ACI 318 Building Code¹ requires that reinforcement be distributed in beams to control crack widths. Conventionally, crack widths are considered only at the extreme tensile face of the beam since the largest crack widths are commonly expected at this location. It has been shown,²⁻⁵ however, that the largest crack widths in some beams may occur in the web along the beam side face. Experimental studies conducted by Beeby² found that the maximum crack width occurs about midheight. Therefore, ACI requires skin reinforcement in beams with effective depths greater than 36 in. to limit the crack width on the side face.

The use of thicker concrete covers has been increasing because research and experience have indicated that the use of thicker covers, as well as high-performance concrete, can increase durability. Since concrete cover has been shown^{6,7} to be a primary variable affecting crack widths, there is concern that current code provisions to control cracking may not be adequate. A review of flexural cracking and its control was undertaken in Reference 7 to examine the impact of increased cover on cracking. This work presented a new formulation of the equation for calculating crack widths based on the physical phenomenon. The research, however, concentrated on crack widths located at the extreme tension face and at the level of the reinforcement. It is the purpose of this paper to investigate the role of cover on side-face cracking and its control.

RESEARCH SIGNIFICANCE

To permit the design and construction of more durable concrete structures, it is important to address the following questions: Can concrete cover be increased while still providing adequate side-face crack control? Are the current design provisions valid for increased covers? Does the cracking model developed previously adequately model side-face cracking? This paper will attempt to answer these questions and provide recommendations for the control of side-face cracking with the use of thicker concrete covers.

DESIGN PROVISION BACKGROUND

The current design provisions for side-face crack control are based primarily on the work of Frantz and Breen.^{3,4} Spurred by the inadequate behavior of several 8 ft deep inverted T-beams, Frantz and Breen performed an experimental and analytical study of the side-face cracking phenomenon. This study tested 44 T-beam reduced-scale beam segments. Based on analysis of the test results, design recommendations were presented for the control of side-face cracking.⁵

Because concrete cover is of primary interest, it is important to examine the range of concrete covers included in testing.^{3,4} Concrete covers over the skin reinforcement were tested ranging from 0.75 to 3.0 in., as shown in Fig. 1. The majority of the tests in the series were conducted with a cover of 1.125 in., with only two specimens tested at 3.0 in. As test data for thicker covers is not available, it is useful to consider a physical model of cracking that is applicable for the side face.

CRACKING MODEL

Previous research developed a physical model for cracking that provided reasonable results for the modeling of cracking at both the bottom tensile face and at the level of the reinforcement. The complete background for the development of the model is available in Reference 7. The physical model will be extended here for the computation of side-face crack widths.

Crack width

Flexural cracking in a beam without skin reinforcement is shown in Fig. 2. The crack width at the level of the primary reinforcement can be calculated as

$$w_c = \epsilon_s S_c \quad (1)$$

where

- w_c = crack width at level of primary reinforcement;
- ϵ_s = reinforcing strain = f_s/E_s ;
- S_c = crack spacing;
- f_s = primary reinforcement stress; and
- E_s = reinforcement modulus of elasticity.

Equation (1) is based on the conservative assumption that the reinforcement is uniformly strained over the crack spacing. The crack width determined from this equation is applicable only at the location of the primary reinforcement. Therefore, the reinforcing stress corresponds to the stress in the primary reinforcement.

ACI Structural Journal, V. 99, No. 3, May-June 2002.

MS No. 01-304 received September 30, 2001, and reviewed under Institute publication policies. Copyright © 2002, American Concrete Institute. All rights reserved, including the making of copies unless permission is obtained from the copyright proprietors. Pertinent discussion will be published in the March-April 2003 ACI Structural Journal if received by November 1, 2002.

ACI member **Robert J. Frosch** is an assistant professor of civil engineering at Purdue University, West Lafayette, Ind. He received his BSE from Tulane University, New Orleans, La., and his MSE and PhD from the University of Texas at Austin, Austin, Tex. He is secretary of ACI Committee 224, Cracking; and a member of Committee 318-C, Safety, Serviceability, and Analysis; 408, Bond and Development of Reinforcement; and 440, Fiber Reinforced Polymer Reinforcement.

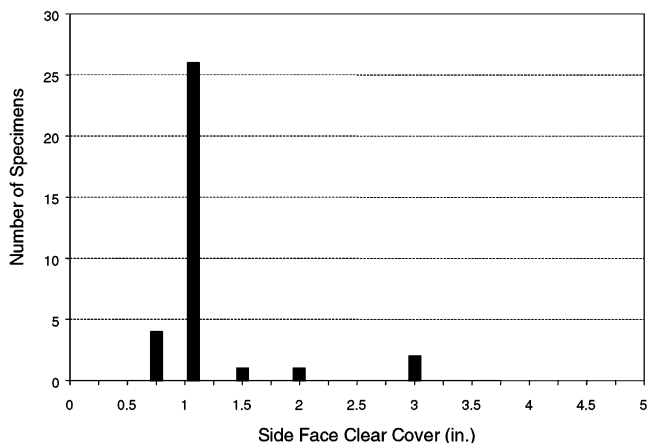


Fig. 1—Side-face cover dimensions.^{3,4}

Strain profile

To determine the crack width over the depth of the beam, it is necessary to consider the strain gradient (Fig. 3). A linear strain gradient is assumed. To determine the crack width at any location z , the crack width determined from Eq. (1) must be multiplied by a strain correction factor β that accounts for the gradient. The correction factor is computed as

$$\beta = \frac{\epsilon_z}{\epsilon_s} = \frac{z - c}{d - c} \quad (2)$$

Assuming that the crack spacing does not vary over the depth of the beam, the largest crack width occurs at the bottom face while the crack width diminishes to zero at the neutral axis. In most beams, however, the crack spacing is not constant over the depth of the beam. Some cracks will extend approximately to the level of the neutral axis, while other cracks will only partially penetrate the beam.

Crack spacing

To calculate the crack width at any location on the cross section, it is necessary to determine the crack spacing at that location. Broms^{8,9} conducted both analytical and experimental studies investigating the spacing of cracks in both pure tension and flexural members. Based on analysis of pure tensile sections, Broms found that the crack spacing is a function of the distance from the reinforcement. It was shown that the minimum theoretical crack spacing is equal to the distance from the point at which the crack spacing is considered to the center of the reinforcing bar located closest to that point. Furthermore, it was found that the maximum theoretical crack spacing is twice the minimum once a stabilized crack pattern has developed, typically around 20 to 30 ksi in the reinforcement being considered. Experiments conducted by Broms⁸ support the analytical findings for tension specimens with covers up to 6 in. Broms also investigated the crack spacing for flexural members (beams).^{8,9} These studies provide insight regarding the formation of flexural cracks and the length of flexural cracks through the cross section.

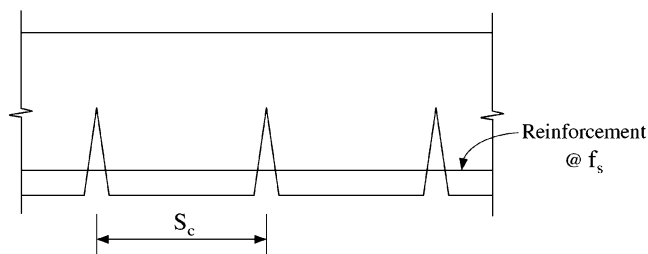


Fig. 2—Beam flexural cracking.

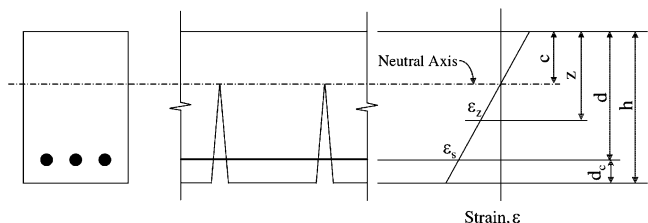


Fig. 3—Strain gradient.

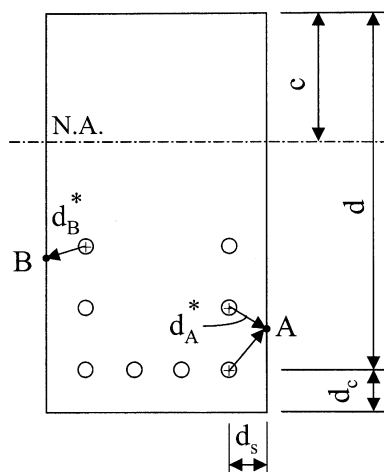


Fig. 4—Controlling distance for beam with skin reinforcement.

Based on the theoretical work presented by Broms,^{8,9} the crack spacing at any location along the depth of the cross section can be calculated as

$$S_c = \psi_c d^* \quad (3)$$

where

- S_c = crack spacing;
- d^* = distance to point being considered;
- ψ_s = crack spacing factor:
 - 1.0 for minimum crack spacing;
 - 1.5 for average crack spacing; and
 - 2.0 for maximum crack spacing.

As illustrated in Fig. 4, the crack spacing at the surface for any given point on the cross section can be calculated. To compute the crack spacing at Point A, the distance d_A^* is computed as the distance to the closest reinforcement. The controlling distance is shown. By multiplying this distance by the appropriate crack spacing factor, the crack spacing at a given location can be determined. Crack spacing at other locations on the cross section, such as Point B, can also readily be calculated.

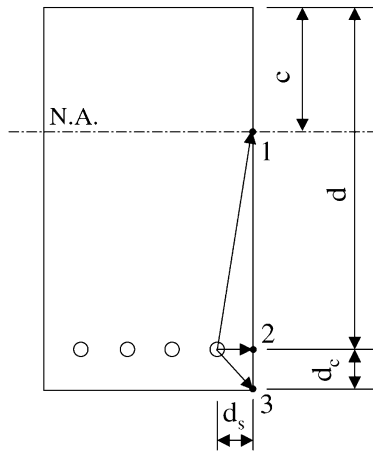


Fig. 5—Controlling distance for beam without skin reinforcement.

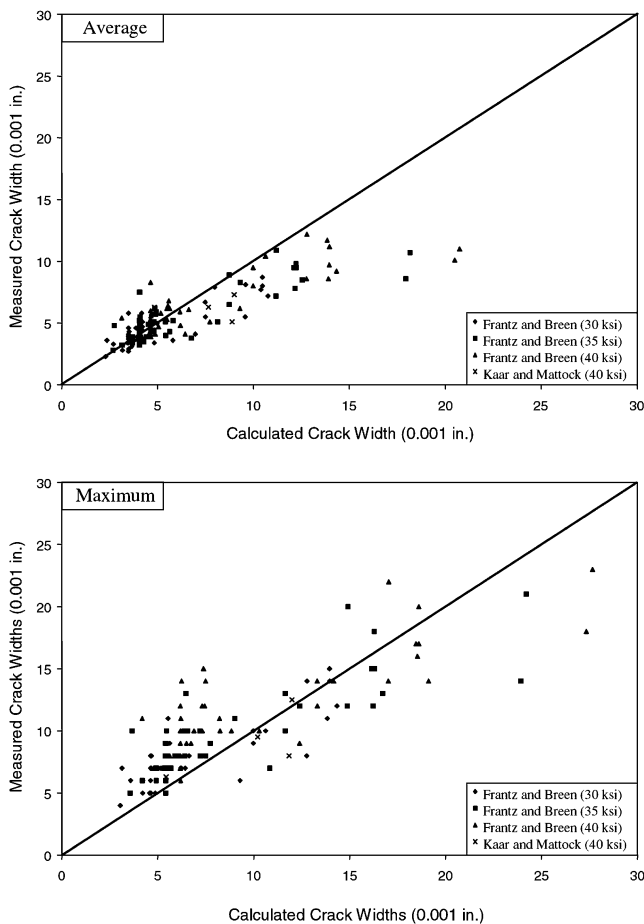


Fig. 6—Side-face crack width results.

Figure 5 shows a cross section that contains only primary reinforcement. For this case, it can be seen that the maximum crack spacing will occur at the neutral axis because this is the largest distance (Point 1, concrete tensile strength neglected), while the smallest crack spacing along the surface will occur at the level of the reinforcement, the shortest distance (Point 2). Point 3 illustrates the appropriate distance used to determine the crack spacing at the bottom face. As larger crack spacings can occur in the web rather than at the bottom face, it is possible for crack widths to be larger within the depth of the cross section, depending on the tensile strain at that level in the

Table 1—Side-face crack width data

Investigator	Reinforcement stress levels, ksi	No. of specimens	No. of observations	
			Average crack width	Maximum crack width
Frantz and Breen	30, 35, and 40	44	126	125
Kaar and Mattock	40	3	6	6
Total	—	47	132	131

Table 2—Comparison results

Specimens	Average crack widths			Maximum crack widths		
	No. of observations	Calculated/measured		No. of observations	Calculated/measured	
		Average	Standard deviation		Average	Standard deviation
Frantz and Breen (30 ksi)	41	1.07	0.27	41	0.85	0.25
Frantz and Breen (35 ksi)	41	1.13	0.31	44	0.86	0.27
Frantz and Breen (40 ksi)	41	1.13	0.32	40	0.85	0.27
Kaar and Mattock (40 ksi)	6	1.20	0.32	6	0.99	0.26
All specimens	132	1.11	0.30	131	0.86	0.26

section. This model illustrates that the crack width in beams with a large depth can be larger than the crack width at the bottom surface. Skin reinforcement provides for a decrease in the crack spacing along the depth of the cross section by decreasing the distance from the closest reinforcement.

CRACK WIDTH ANALYSIS

Crack widths calculated based on the physical model presented were compared with test data from Frantz and Breen³ and Kaar and Mattock.¹⁰ Kaar and Mattock also tested a limited number of specimens containing skin reinforcement (Series 1: Highway Bridge Girders). This data set was used to determine the applicability of the model presented previously to account for side-face cracking. Research presented in Reference 7 illustrated the applicability of the physical model in calculating bottom-face crack widths as well as side-face crack widths at the level of the reinforcement.

Crack modeling

The test data included in the analysis are presented in Table 1. The reinforcement stress levels, as well as the number of observations for both average and maximum crack widths, are noted. To evaluate the accuracy of the proposed method, the measured crack widths were plotted versus the computed crack widths. Figure 6 presents the results for both average and maximum crack widths. In general, these figures illustrate that the model reasonably calculates both average and maximum crack widths. The model tends to overestimate average crack widths while underestimating the maximum crack width, especially for the smaller crack widths presented in the graph. A statistical summary comparing the calculated and measured crack widths is provided in Table 2. On average, the physical model overestimated the average crack width by

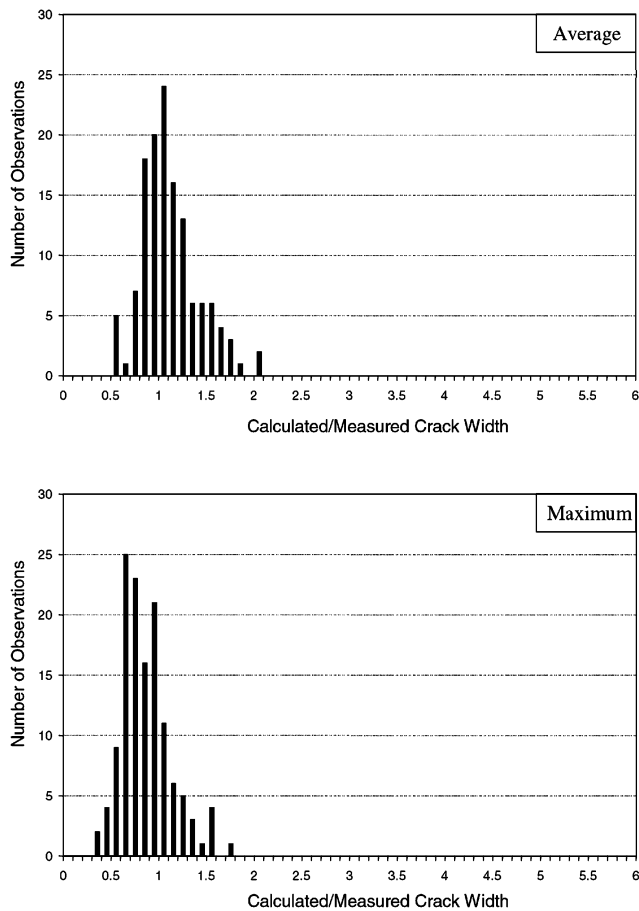


Fig. 7—Side-face crack width comparison.

11%, while it underestimated the maximum crack width by 14%. It can also be seen from the Frantz and Breen tests that the average and standard deviation are approximately the same regardless of the primary reinforcement stress level.

To provide another view of the accuracy of the calculation method, a histogram is presented in Fig. 7 for both average and maximum crack widths. The average crack width results again show that the model is satisfactory. The majority of observations are located around 1.0. In addition, considering the scatter inherent in crack widths (it has commonly been noted that the scatter in crack widths is in the range of 50%), the model is fairly accurate. A comparison of the average and maximum crack width results indicates that the scatter in the results is very similar. The physical model is also fairly accurate for calculating maximum crack widths. It should be noted, however, that the histogram is slightly shifted to the left, which indicates that the measured maximum crack widths for the majority of observations were slightly higher than calculated. The shift corresponds with approximately a 1/3 increase in the measured crack width over the calculated value.

To provide perspective on the accuracy of the calculation for side-face cracking, it is instructive to compare it with the data obtained in the review of bottom face cracking presented in Reference 7 (Fig. 8). As can be seen, the scatter in the data is fairly similar for both average and maximum crack widths. The majority of the data is within the range of 0.5 to 1.5. This comparison indicates that the computation method provides reasonable estimations for the computation of side-face crack widths. Depending on the conservatism desired in calculating maximum side-face crack widths, the crack widths computed

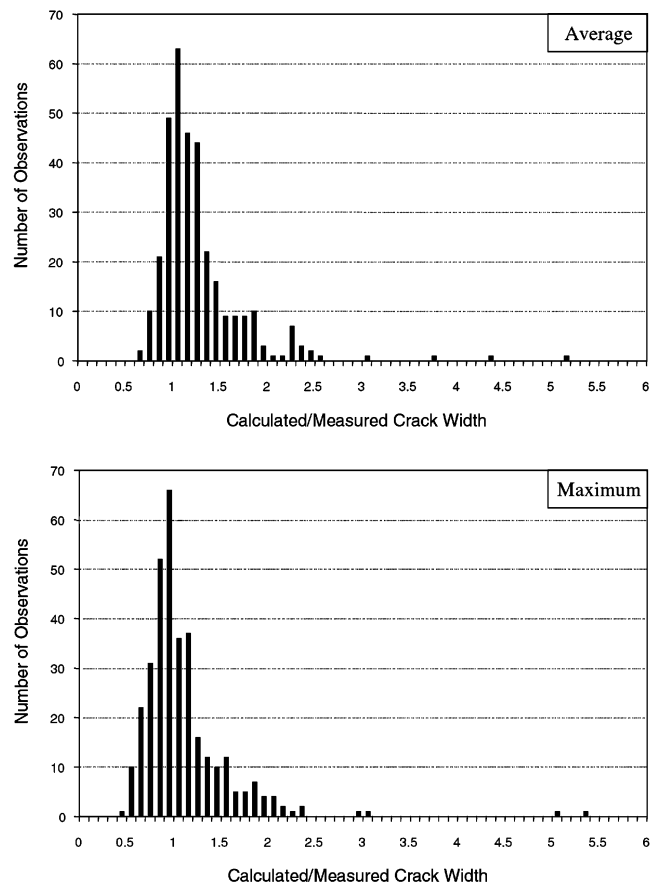


Fig. 8—Bottom-face crack width comparison (from Reference 7).

by the model can be increased. A 1/3 (33%) increase seems appropriate for the results compared here.

Since the primary objective of this research was to investigate the role of side-face cover, a comparison of test results with varying cover was also conducted. This series of specimens from the Frantz-Breen study (Series C) contained T-beams that were designed to be identical except for the skin reinforcement clear cover, which varied from 0.75 to 3.0 in. ($d_s = 0.875$ in. – 3.125 in.). Figure 9 indicates that the physical model accounts for the trend of the data for varying side-cover dimensions for both average and maximum crack widths. For maximum crack widths, two calculated curves are plotted, one for the calculated maximum, and one for a 1/3 increase in the calculated maximum, as recommended previously. From these data, it can be seen that the measured maximum widths fall between these ranges. It is important to note that the measured maximum crack widths were reported to an accuracy of 0.001 in. by nature of the measuring device. As is evident in Fig. 9, an accuracy of ± 0.001 in. can provide a significant adjustment to the vertical position of the data point for the small crack widths measured. In fact, for a 6-mil (0.006 in.) crack reading, there is the potential for a 20% change in result.

Crack width profile

Although the crack width is typically of concern, it is also useful to have information regarding the location of the maximum crack width. Because the crack model allows calculation of the crack width at any location along the cross section, it is possible to construct a profile of the crack

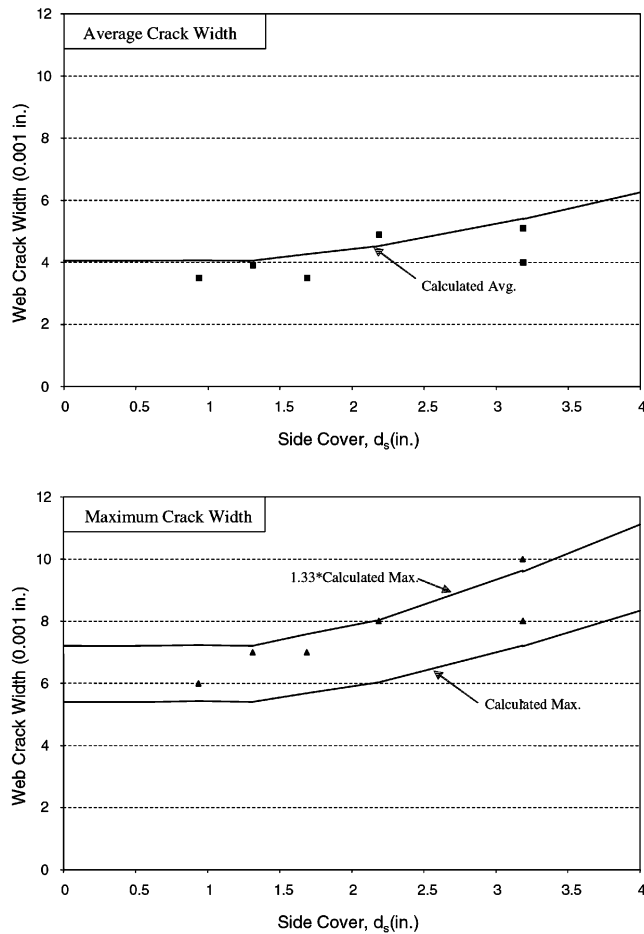


Fig. 9—Skin reinforcement cover comparison.

width through the depth of the section. This profile provides a view of the overall cracking behavior. It also provides information regarding optimum locations to place skin reinforcement for control of side-face crack widths.

Figure 10 illustrates a 36 in. deep beam that contains only primary steel reinforcement. The strain ϵ , crack spacing S_c , and resulting crack width ϵS_c were computed at sections along the side face of the member for a primary reinforcement stress of 35 ksi. The model indicates that the crack width is zero at the neutral axis, and increases toward the bottom face until a maximum is reached. The maximum width occurs along the side face at a location of 11.7 in. from the neutral axis, which is approximately halfway between the neutral axis and the level of the reinforcement ($0.51(d - c)$). Below this point, it is noticed that the crack width decreases until the level of the reinforcement is reached. Below the reinforcement, the crack width once again increases. The influence of the reinforcement can clearly be seen. This behavior is consistent with that observed in the Franz-Breen study as well as that observed in the study by Beeby.²

Figure 11 shows an illustration for the same beam that contains skin reinforcement. The crack width is controlled at the locations of the reinforcement. Between the skin reinforcement, peaks are noted. Assuming that the spacing of the skin reinforcement is constant, there are three possible locations for the point of maximum crack width on the side face. The first point (Point 1) is located at the bottom face, the second (Point 2) is located approximately halfway between the primary reinforcement and the first level of skin reinforcement, and the third (Point 3) is located approximately halfway between

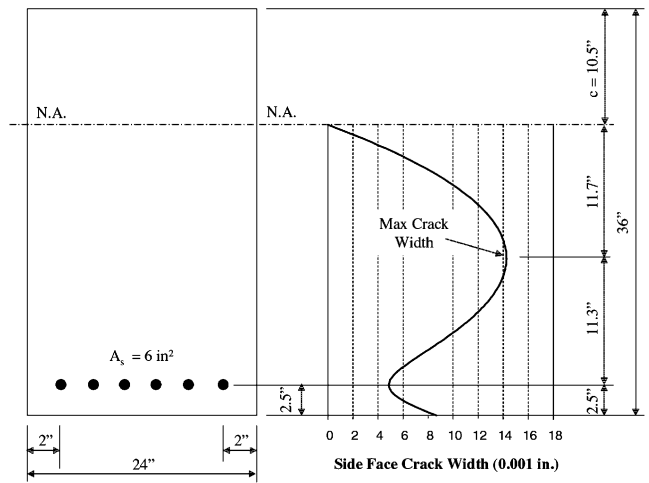


Fig. 10—Crack width profile without skin reinforcement ($f_s = 35$ ksi.).

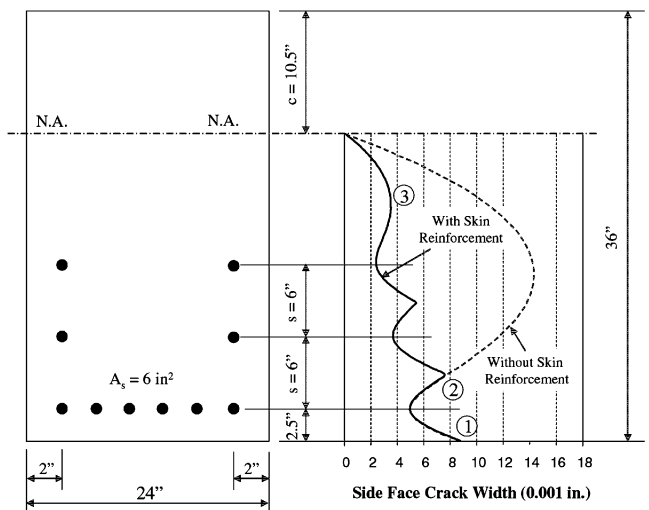


Fig. 11—Crack width profile with skin reinforcement ($f_s = 35$ ksi.).

the last level of skin reinforcement and the neutral axis. For comparison, the crack widths are also plotted for the beam without skin reinforcement.

By understanding the general crack width profile for both sections with and without skin reinforcement, as well as the locations where maximum crack widths can be expected, it is possible to develop methods that provide maximum crack control.

CRACK CONTROL

The cracking model illustrates that the crack spacing and crack width along the side face are functions of the distance from the reinforcement. Therefore, crack control can be achieved by the inclusion of skin reinforcement and by limiting the reinforcement spacing. The concrete cover over the skin reinforcement is also of primary importance. Depending on the depth of the section and the crack widths considered acceptable, however, it may not be necessary to include skin reinforcement.

When to include skin reinforcement?

An analysis was performed on the section shown in Fig. 12. In particular, it was desired to determine the section depth d

such that the maximum crack width does not exceed a limiting value. The value selected as the maximum crack width was 0.016 in., which is the basis for the current crack control provisions in ACI 318-99.¹ Based on the model previously presented, the following equations can be written

$$\epsilon_x = \left(\frac{\epsilon_s}{d-c} \right) x \quad (4)$$

$$S_c = 2\sqrt{d_s^2 + (d-c-x)^2} \quad (5)$$

$$w_s = \epsilon_x S_c \quad (6)$$

The maximum crack spacing and resulting side-face crack width w_s were computed using a crack spacing factor of 2.0, as shown. As previously illustrated in Fig. 9, the maximum crack width may be expected to be up to one-third greater. For the limiting value of 0.016 in. used here, that translates into maximum crack widths in the range of 0.016 to 0.021 in. Since crack widths are primarily an aesthetic issue^{7,11} and considering the scatter inherent in crack widths, a one-third increase was deemed acceptable. This permissible increase is also consistent with the previous research on maximum tensile-surface crack widths.⁷ Therefore, crack widths for all analyses were computed using the 2.0 crack spacing factor.

The maximum crack width has previously been shown to be located at approximately halfway between the reinforcement and the neutral axis $x \approx \frac{d-c}{2}$. The exact location is slightly below (less than a 1%² difference), and does not improve the results. If Eq. (4) through (6) are combined and solved at $x = \frac{d-c}{2}$, the following equation results

$$w_c = \epsilon_s \sqrt{d_s^2 + \left(\frac{1}{2}(d-c) \right)^2} \quad (7)$$

This equation can be solved for d as a function of d_s . The neutral axis dimension c is primarily a function of the reinforcement percentage ρ . The concrete strength provides only a minor influence, as it affects the modulus of elasticity. For 5,000-psi concrete, c can range from 0.23 to 0.37 d for $\rho = 0.5$ to 1.5%, respectively. Therefore, $c = 0.3d$ was used as a commonly assumed and typical value. The results from analyses for primary reinforcement stress levels of 36 and 45 ksi (typical service load stresses of Grade 60 and Grade 75 steel, respectively) are presented in Fig. 13. From the 36-ksi curve, it can be seen that for concrete side face covers up to 3 in., it is possible to construct sections with an effective depth up to 36 in. without the use of skin reinforcement. For greater cover dimensions, the maximum effective depth that does not require skin reinforcement should be decreased. Alternately, the addition of skin reinforcement can be used to control crack widths.

For design purposes, simplified curves are presented indicating the effective beam depths that do not require skin reinforcement. As shown, for Grade 60 reinforcement, there is a reduction in the maximum effective depth for covers beyond 3 in. For the majority of structures, the cover will be less than 3 in., which results in a maximum $d = 36$ in. This value is consistent with the current design requirements of ACI 318-99.¹

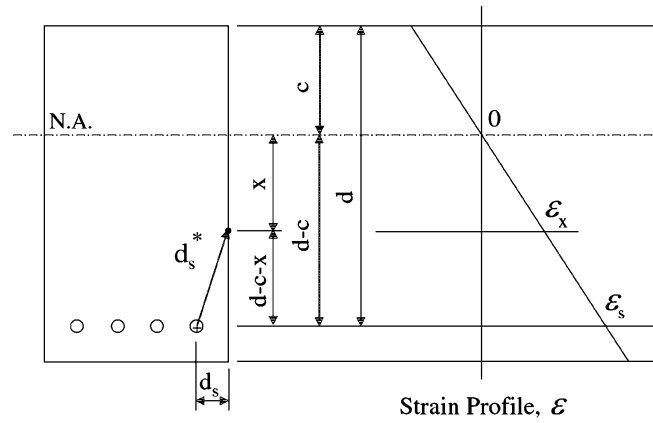


Fig. 12—Beam cross section (elimination of skin reinforcement.)

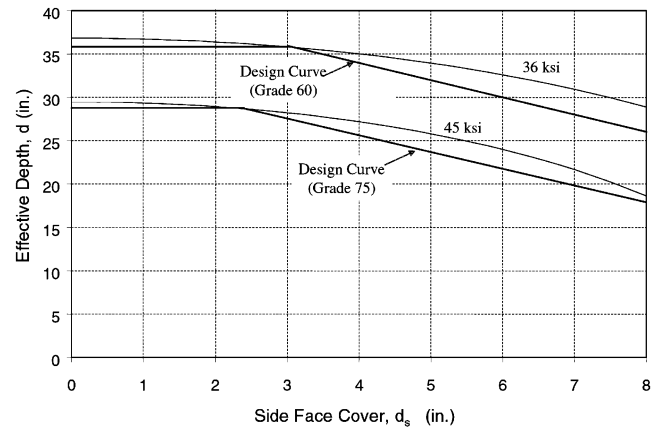


Fig. 13—Skin reinforcement elimination.

Skin reinforcement spacing

For sections where skin reinforcement is required, it is useful to determine the maximum spacing of the reinforcement that maintains control of the crack width through the section depth. Using a maximum crack width of 0.016 in., the maximum reinforcement spacing was determined. The case investigated is shown in Fig. 14. The following equations can be written

$$\epsilon_x \approx \epsilon_s = \frac{f_s}{E_s} \quad (8)$$

$$S_c = 2\sqrt{d_s^2 + x^2} \quad (9)$$

$$w_s = \epsilon_x S_c \quad (10)$$

As was previously discussed, for a constant spacing of skin reinforcement, the placement of the first bar is the most critical. The crack width was calculated halfway between the primary reinforcement and the first skin reinforcement ($x = s/2$), since this location is approximately the maximum (less than 1% difference). In addition, it was conservatively assumed that the strain at this location is the same as at the primary reinforcement. The combination of Eq. (8) through (10) resulted in

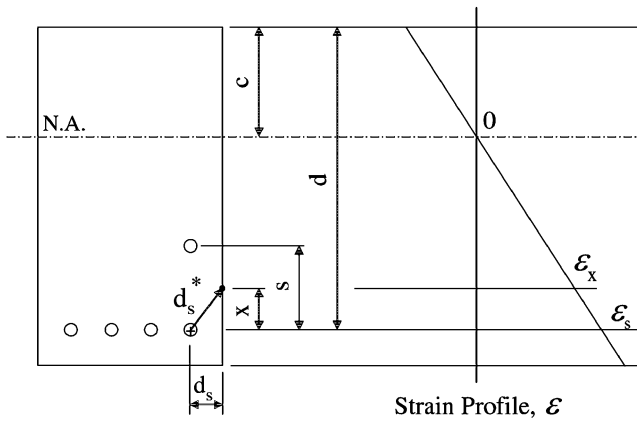


Fig. 14—Beam cross section (skin reinforcement spacing).

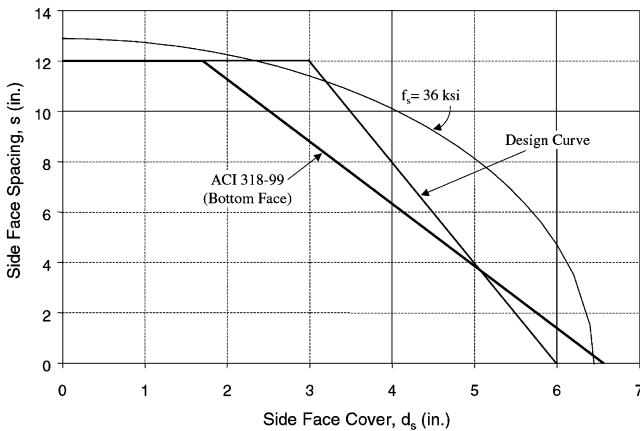


Fig. 15—Skin reinforcement spacing.

$$w_s = 2 \frac{f_s}{E_s} \sqrt{d_s^2 + \left(\frac{s}{2}\right)^2} \quad (11)$$

For a given service load stress f_s the maximum bar spacing was computed. The results of this analysis for Grade 60 steel (service stress = 36 ksi, $E_s = 29,000$ ksi) are shown in Fig. 15. It can be seen that the maximum skin reinforcement spacing is a function of the concrete cover over the skin reinforcement. In addition, a simplified design curve is also shown. The results indicate that a maximum bar spacing of 12 in. will provide reasonable crack control up to 3 in. of concrete cover. The design curve presented is consistent with the design recommendations that were proposed in Reference 7 for reinforcement located at the beam bottom face. Also shown are the ACI 318-99¹ design provisions for the distribution of reinforcement at the beam bottom face. These reinforcement provisions are shown to also provide adequate control of cracking along the side face. Therefore, the ACI provisions for bottom-face reinforcement can also be used for the design of skin reinforcement. This unification can provide simplification of the current design provisions as well as take into account the effect of the concrete cover.

How far to extend skin reinforcement?

For sections where skin reinforcement is provided, it is also necessary to determine the location in the section where the reinforcement can be discontinued. Using a maximum crack width of 0.016 in., an analysis was conducted of the

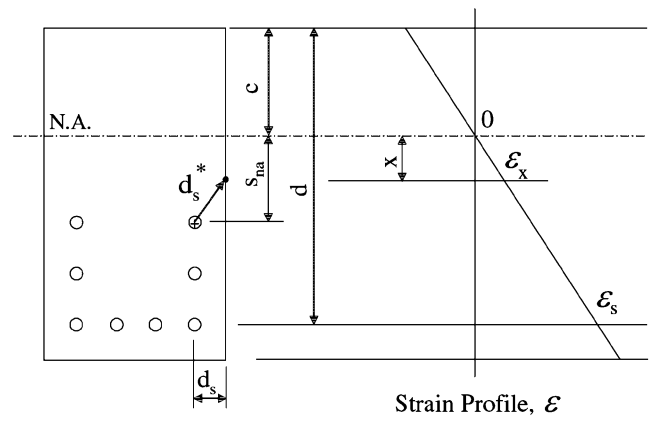


Fig. 16—Beam cross section (skin reinforcement termination point).

beam shown in Fig. 16. Since crack widths are controlled by skin reinforcement below its termination point, it is desired to calculate the maximum distance s_{na} where the skin reinforcement can be eliminated. The following equations can be written for the crack width computed at the location x

$$\epsilon_x = \left(\frac{\epsilon_s}{d-c}\right)x \quad (12)$$

$$S_c = 2\sqrt{d_s^2 + (s_{na} - x)^2} \quad (13)$$

$$w_s = \epsilon_x S_c \quad (14)$$

The maximum crack width will occur approximately halfway between the neutral axis and the location of the first layer of skin reinforcement at a distance $(x = \frac{s_{na}}{2})$ from the neutral axis. Equation (12) through (14) were combined, which resulted in

$$w_s = s_{na} \left(\frac{\epsilon_s}{d-c}\right) \sqrt{d_s^2 + \left(\frac{s_{na}}{2}\right)^2} \quad (15)$$

As in previous analyses, the neutral axis location was assumed to be $c = 0.3d$. Therefore, for a given strain level of the primary reinforcement, only two variables remain, d and d_s . Figure 17 presents the results of analyses conducted for $d_s = 1.5$ in. (typical design value) at working stress levels of 36 and 45 ksi. The analysis results are presented as $((d - (c + s_{na}))/d)$ versus the beam effective depth. The quantity $(d - (c + s_{na}))/d$ is shown, since this value physically represents the percentage of cross section measured from the tensile reinforcement that requires skin reinforcement. For beam depths across a wide spectrum, it can be seen that, conservatively, skin reinforcement is only required within the bottom 40% of the cross section. Similar analyses were performed for varying concrete cover dimensions d_s ranging from 1 to 4 in. These analyses indicated that changes in d_s do not significantly change the results. In fact, the results are practically identical for this range of cover and indicate that concrete cover does not affect the results. Therefore, it is reasonable and conservative to require skin reinforcement in the tension zone for 50% of

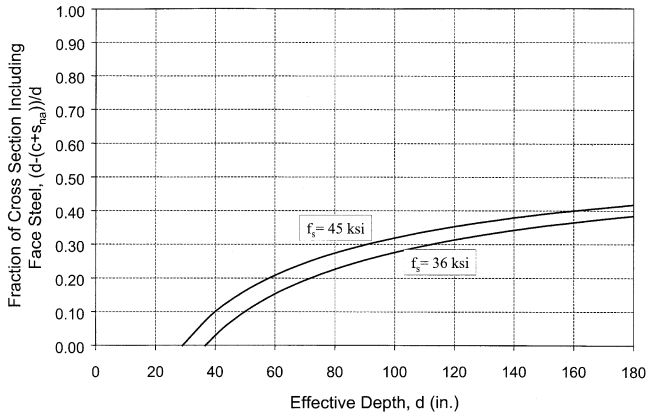


Fig. 17—Skin reinforcement termination.

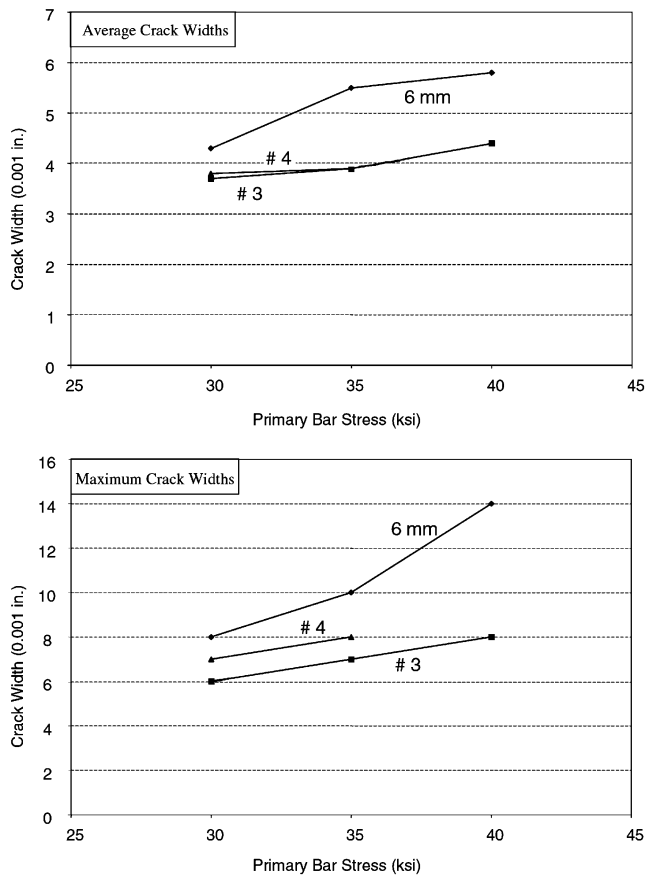


Fig. 18—Bar size effect on side-face crack widths.

the effective depth. This recommendation is consistent with the current ACI requirements.

Reinforcement size

All of the analyses presented previously do not mention the size of the reinforcement that is required to control side-face cracking. In reviewing the physical model, it can be seen that the size of the reinforcement does not directly enter the equations. The only impact bar size makes is by changing the dimension d_s . Since changes in the bar diameter do not significantly change the value of d_s , the bar size does not significantly affect crack widths. This effect of bar size was

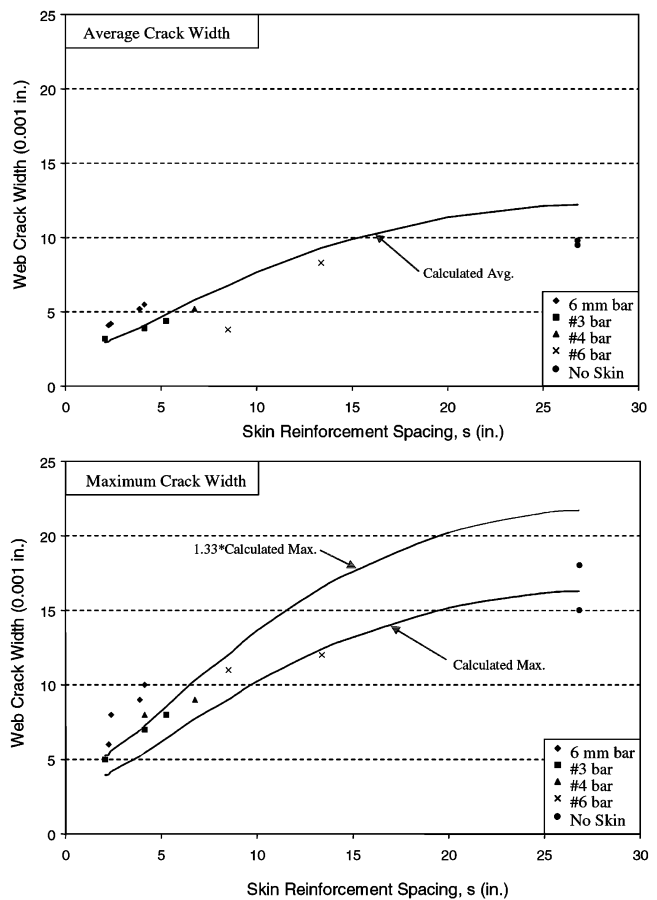


Fig. 19—Effect of skin reinforcement spacing and bar size ($f'_s = 35$ ksi).

also noted by Gergely and Lutz:⁶ “the bar diameter is not a major variable” in the factors affecting crack width.

The physical model assumes that plane sections remain plane. Therefore, the strains must be compatible regardless of reinforcement size. The primary effect of the reinforcement is to control the crack spacing at the beam surface. Frantz and Breen⁴ also recognized this effect in one of their conclusions: “skin reinforcement affects only a narrow strip of concrete along each side face of the web.” By providing a reasonable distribution of reinforcement, crack spacing can be controlled, which results in control of the crack width.

To provide experimental evidence, a series of test specimens from Frantz and Breen³ were analyzed. These specimens (A7, A8, and A9) held all dimensions constant except for the size of the skin reinforcement. Therefore, they provide good insight into the effect of reinforcement size. The measured crack widths are presented versus the primary reinforcement stress (Fig. 18) for both average and maximum crack widths. As noted from both average and maximum crack widths, the 6 mm bars produced the largest crack widths. The No. 4 bars, however, produced approximately the same or slightly larger crack widths as compared with the No. 3 bars. These tests results tend to support the fact that the size of the bar does not affect the crack width.

It should be noted that the 6 mm bars used in the tests were Swedish deformed Grade 77 bars. This is significant in that the deformations on these bars are not as pronounced as those of the No. 3 and No. 4 bars that conformed to the ASTM A615 standard on bar deformations. It is possible that the 6 mm bars did not bond as well as the No. 3 and No. 4

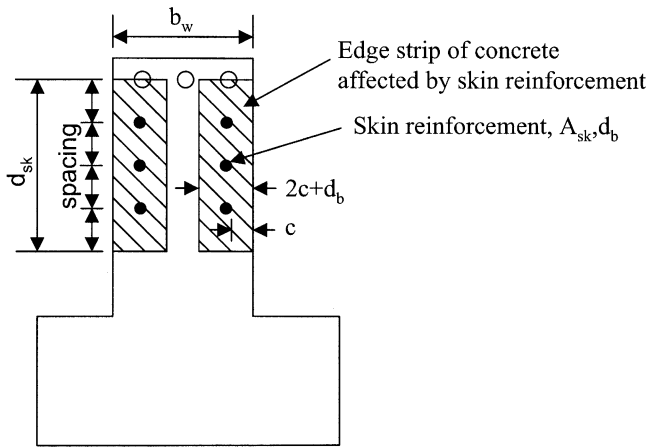


Fig. 20—Skin reinforcement ratio variables (from Reference 4).

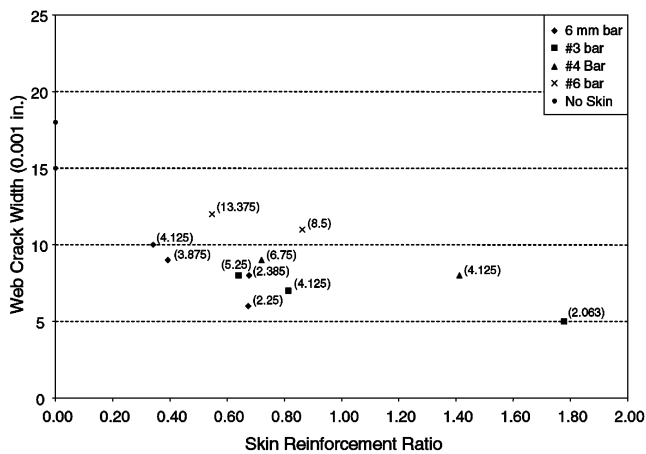


Fig. 21—Crack width versus skin reinforcement ratio (maximum crack widths).

bars, which would result in a wider crack spacing and larger crack widths for specimens utilizing these bars.

To provide further evidence regarding the effect of bar size, additional test data from Frantz and Breen³ (Series A) was reviewed. These specimens, except Specimen A-15 (excluded from the analysis), held all variables constant except for the spacing and size of the skin reinforcement. If it is assumed that the bar size does not affect crack width, the crack width should be controlled only by the skin spacing for a given stress level (clear concrete cover held constant). It should be noted that Specimen A-14 was also excluded from the analysis because the skin reinforcement was discontinued less than halfway up the side face.

The measured crack widths are presented versus the skin-reinforcement spacing for both average and maximum crack widths in Fig. 19 at a primary reinforcement stress of 35 ksi. The calculated crack widths are also presented. Specimens containing no skin reinforcement (Specimens A-1-0 and A-2-0) are plotted at a skin reinforcement spacing of 26.8 in., which coincides with the location of the neutral axis. A review of the average crack-width plot indicates that the specimens follow the calculated curve fairly well. The No. 3 and No. 4 bars follow the calculated curve very well and do not appear to indicate an effect of bar size. The 6 mm bar provides a slightly higher crack width than the calculated, while the No. 6 bar provides a slightly lower crack width, especially for the specimen with a reinforcement spacing of 8.5 in.

(Specimen A-13). This trend suggests that there may be some benefit in using a larger bar. However, when reviewing the maximum crack width, which is typically of concern, Specimen A-13 fits well with the other data. In general, the specimens reinforced with No. 3, No. 4, and No. 6 bars follow the calculated curves, which supports the theory that the bar size does not affect crack width. The physical model provides reasonable estimates of crack width regardless of skin reinforcement size. As previously discussed, the 6 mm bars produce slightly higher crack widths, which may be related to bonding characteristics.

Based on this background, it does not appear that the bar size significantly affects the crack width. Therefore, as long as the skin reinforcement provides adequate bond transfer to the concrete, any size bar can be used successfully. It is highly recommended that deformed bars be used for this purpose because bond transfer is essential for the control of crack widths.

The finding that bar size does not significantly affect crack widths seems opposed to results in Reference 3, which indicates a relationship between the percentage of skin reinforcement (including bar size) and side-face crack width. In general, as the skin reinforcement ratio increases, the crack width was observed to decrease. The skin reinforcement ratio ρ_{sk} can be defined as Eq. (16), while the variables are defined in Fig. 20.

$$\rho_{sk} = \frac{\text{Total } A_{sk}}{2(2c + d_b)d_{sk}} \quad (16)$$

The skin reinforcement ratio combines the effect of bar area, cover, and reinforcement spacing; therefore, the effect of each variable cannot be assessed. As the skin spacing is decreased, the total area of skin reinforcement (Total A_{sk}) increases, resulting in an increase of the skin reinforcement ratio. The reinforcement spacing can also affect d_{sk} ; however, its value depends primarily on the skin termination location. For a decrease in the skin reinforcement spacing, both the physical model and the skin reinforcement ratio relationship agree that the crack width should decrease. Therefore, upon closer examination, the physical model does not contradict the general trend between the skin reinforcement ratio and crack width.

The maximum measured crack width for Series A specimens was also plotted versus the skin reinforcement ratio in Fig. 21. The skin spacing, in in., is noted next to each data point. For a given bar size, a trend between skin reinforcement ratio (also bar spacing) and crack width can be noted. However, by including the effect of bar size in ρ_{sk} (an increase in bar size increases the total A_{sk} and ρ_{sk}), scatter is introduced. As the bar size was increased at a constant skin reinforcement ratio (for example, at approximately $\rho_{sk} = 0.80$), the crack width also increased. Based on review of this data, it was found that the general relationship between the skin reinforcement ratio and the crack widths noted in Reference 3 can be attributed primarily to the effect of the skin reinforcement spacing on ρ_{sk} and not to changes in bar size. This again supports the finding that the skin reinforcement spacing is the primary parameter that should be controlled.

CONCLUSIONS

To control side-face cracking for structures with larger covers (greater than 3 in.), the current design provisions are at a disadvantage because they were based on test results

with clear cover dimensions ranging from 0.75 to 3 in., with the majority of tests conducted at 1.125 in. This paper extends a physical model presented in Reference 7 for use in the calculation of crack widths at any location along the beam surface. Use of this model is supported by an evaluation of the existing test data. The resulting equations were used to develop solutions for the control of side-face cracking in reinforced concrete structures. It was found that side-face crack widths can be controlled through the spacing of skin reinforcement using the same spacing requirements as those used for the control of bottom-face cracks.

Design recommendations

Based on the physical model, the following design recommendations are presented that address the control of cracking in reinforced concrete structures. These recommendations also aim to unify the design provisions for the control of side-face cracking as well as bottom-face cracking. The recommended design curves for Grade 60 reinforcement are illustrated in Fig. 13 and 15.

1. The maximum spacing of flexural tension reinforcement shall be given by

$$s = 12\alpha_s \left[2 - \frac{d_c}{3\alpha_s} \right] \leq 12\alpha_s$$

$$\alpha_s = \frac{36}{f_s}; \text{ and}$$

2. Skin reinforcement shall be required along both side faces of a member for a distance $d/2$ nearest the flexural tension reinforcement if the effective depth exceeds the value

$$d = 42\alpha_s - 2d_c \leq 36\alpha_s$$

where

d = effective depth, in.;

d_c = thickness of concrete cover, in., for bottom-face reinforcement, measured from extreme tension fiber to center of bar, and for skin reinforcement, measured from side face to center of bar;

f_s = calculated stress in primary reinforcement at service load, kips/in.², shall be computed as the unfactored moment divided by the product of steel area and internal moment arm. It shall be permitted to take f_s as 60% of specified yield strength f_y ;

s = maximum spacing of reinforcement, in.; and

α_s = reinforcement stress factor.

CONVERSION FACTORS

1 in.	=	25.4 mm
1 kip	=	4.448 kN
1 ksi	=	6.895 MPa

REFERENCES

1. ACI Committee 318, "Building Code Requirements for Structural Concrete (ACI 318-99) and Commentary (ACI 318R-99)," American Concrete Institute, Farmington Hills, Mich., 1999, 391 pp.
2. Beeby, A. W., "An Investigation of Cracking on the Side Faces of Beams," *Technical Report* No. 42.466, Cement and Concrete Association, London, Dec. 1971, 11 pp.
3. Frantz, G. C., and Breen, J. E., "Control of Cracking on the Side Faces of Large Reinforced Concrete Beams," *Research Report* 198-1F, Center for Highway Research, University of Texas at Austin, Sept. 1978, 242 pp.
4. Frantz, G. C., and Breen, J. E., "Cracking on the Side Faces of Large Reinforced Concrete Beams," *ACI JOURNAL, Proceedings* V. 77, No. 5, Sept.-Oct. 1980, pp. 307-313.
5. Frantz, G. C., and Breen, J. E., "Design Proposal for Side Face Crack Control Reinforcement for Large Reinforced Concrete Beams," *Concrete International*, V. 2, No. 10, Oct. 1980, pp. 29-34.
6. Gergely, P., and Lutz, L. A., "Maximum Crack Width in Reinforced Concrete Flexural Members," *Causes, Mechanism, and Control of Cracking in Concrete*, SP-20, Robert E. Philleo, ed., American Concrete Institute, Farmington Hills, Mich., 1968, pp. 87-117.
7. Frosch, R. J., "Another Look at Cracking and Crack Control in Reinforced Concrete," *ACI Structural Journal*, V. 96, No. 3, May-June 1999, pp. 437-442.
8. Broms, B. B., "Crack Width and Crack Spacing in Reinforced Concrete Members," *ACI JOURNAL, Proceedings* V. 62, No. 67, Oct. 1965, pp. 1237-1255.
9. Broms, B. B., "Stress Distribution in Reinforced Concrete Members with Tension Cracks," *ACI JOURNAL, Proceedings* V. 62, No. 65, Sept. 1965, pp. 1095-1108.
10. Kaar, P. H., and Mattock, A. H., "High-Strength Bars as Concrete Reinforcement—Part 4: Control of Cracking," *Journal, PCA Research and Development Laboratories*, V. 5, No. 1, Jan. 1963, pp. 15-38.
11. Gergely, P., "Role of Cover and Bar Spacing in Reinforced Concrete," *Significant Developments in Engineering Practice and Research: A Tribute to Chester P. Siess*, SP-72, Mete A. Sozen, ed., American Concrete Institute, Farmington Hills, Mich., 1981, pp. 133-147.